JOURNAL OF MATERIALS SCIENCE 4 (1969) 734–742

Growth, Perfection and Antiferromagnetic Domain Structure of Epitaxial Cobalt Oxide

F. J. SPOONER, M. W. VERNON
Physics Department, Royal Military College of Science, Shrivenham, Swindon, Wilts, UK

Received 31 March 1969

Uniform single crystals of cobalt oxide have been grown over a wide range of temperature (210° C) by vapour hydrolysis of cobalt bromide on to (001) cleavage faces of magnesium oxide. Thicker crystals have been grown by this technique than previously reported, and the dependence of the growth on the experimental parameters is presented.

Optical and X-ray topographic techniques have been used to study the distribution of imperfections and antiferromagnetic domains in these crystals. The appearance of plastic deformation at the growth surface in crystals grown at high temperatures is a result of the combined stresses induced by differential thermal contraction of overgrowth and substrate, and the presence of growth striations throughout the bulk of the crystals. The complexity of the antiferromagnetic domain structure, which is sensitive to crystal thickness, is a direct result of the inhibiting effect of the substrate and the misfit associated with the antiferromagnetic tetragonal distortion.

These results on cobalt oxide are compared and contrasted to those previously reported on nickel oxide grown under similar conditions.

1. Introduction

Cobalt oxide, in common with some other transition metal oxides, is an antiferromagnetic material with a Néel temperature T_N of 290° K. Above this temperature it is paramagnetic with the rocksalt structure, whilst below, antiferromagnetic ordering results in a tetragonal distortion of the lattice [1]. Each (1 1 1) plane has a ferromagnetic arrangement of spins, the spin direction being approximately along ⟨0 0 1⟩, and alternate (1 1 1) planes have antiparallel arrangements. The tetragonal distortion is a result of a contraction (1.03% at −180° C) along one of the original cubic axes (parallel to the appropriate ⟨0 0 1⟩ spin direction), and a smaller expansion (0.13% at − 180° C) along the other two axes. This can give rise to a twin domain structure, where adjacent domains have different contraction axes, and the spin directions in adjacent domains are twin related about the twin wall (usually denoted T wall).

Previous work by the present authors [2, 3] on nickel oxide gave a detailed account of the epitaxial growth of this oxide, the effects of the growth parameters on the structural perfection and morphology of these crystals, and the effect of the magnesium oxide substrate on the residual strain, plastic deformation and antiferromagnetic domain structure. The fundamental differences between CoO and NiO are: (i) at normal room temperature, CoO is just paramagnetic and cubic (T_N = 290° K), whilst NiO is antiferromagnetic and rhombohedral (T_N = 523° K); (ii) at the growth temperature, the lattice constant of CoO is greater than that of the MgO substrate, whilst that of NiO is less; and (iii) the tetragonal distortion of CoO results in the formation of three types of antiferromagnetic domain, whilst the rhombohedral distortion of NiO gives four types of domain. All these factors play a part in the final appearance of the epitaxial crystals after cooling from the growth temperature.

The purpose of the work in this paper is to compare and contrast the epitaxial growth, structural perfection and antiferromagnetic domain structure of CoO with that of NiO.

2. Epitaxial Growth

2.1. Experimental

This investigation into the characteristics of growth of epitaxial CoO, by vapour hydrolysis of cobalt bromide onto (001) cleavage faces of MgO, follows a similar pattern to that described previously by the present authors on epitaxial NiO [3], and the experimental arrangement was identical. The quantitative variation of crystal thickness, surface morphology and growth rate with substrate temperature and bromide vapour pressure (p_B) was examined in both the open and closed systems (open and closed refers to the bromide enclosure as explained in [3]). No data was available for the vapour pressure of $CoBr_2$ as a function of temperature and, consequently, no quantitative examination of growth thickness as a function of bromide vapour pressure could be made.

2.2. Results and Discussion

2.2.1. Open System

The variation of thickness with temperature using a fixed quantity of cobalt bromide at a water vapour pressure of 25 mm is shown in curve A of fig. 1. The mass of bromide used was 8.5 g and the mass of the deposit at T_M was 0.17 g, representing an efficiency of 12.5% for conversion of bromide to epitaxially deposited oxide. The shape of the curve up to T_M is similar to that for NiO [3], and the thicknesses are comparable to that of NiO. This is a significant feature, since other workers growing epitaxial CoO by similar techniques report much lower values for maximum thickness [4–6]. However, the thickness does fall off much more quickly beyond T_M than in the NiO growth, the main reason being the low melting point of cobalt bromide (678° C), which is only slightly higher than T_M. In general the deposit thickness is uniform across the substrate, as was the case in NiO.

Although the vapour pressure of solid $CoBr_2$ as a function of temperature is unknown, it is likely to be similar to $NiBr_2$, and it is reasonable to expect a linear region of increase of thickness with bromide vapour pressure extending up to T_M, with slower variation at high and low vapour pressures for the same reasons as in NiO, enhanced above T_M by liquid $CoBr_2$ escaping from the enclosure. Measurements of the growth rate of CoO revealed an exponential variation with reciprocal temperature with an overall activation energy of 36.2 kcal/mol over the whole temperature range. Although this value is slightly higher than the 31.5 kcal/mol for NiO, it is close enough to assume that the same rate limiting process is dominant in both cases.

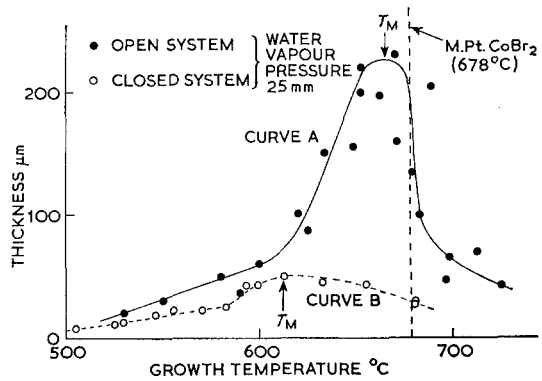

Figure 1 Variation of thickness as a function of growth temperature.

The surface morphology of the CoO was similar to that observed in NiO, inasmuch that the surfaces were smooth with a mosaic of small angle boundaries over the range of good growth. However, the temperature range over which this occurred (600 to 660° C) was much less than that for NiO, the CoO surfaces being much more susceptible to changes in water vapour pressure (p_w) and total ambient pressure. At lower temperatures (higher p_w), the surfaces were extremely pitted, and above T_M (higher p_B), the surfaces were covered with regular flat-topped "hillocks" which were considerably etched.

No sign of growth spirals were seen on any of the CoO crystals, although Greiner *et al* [6] reported that their CoO surfaces were covered with spiral growth pyramids. However, these authors used polished MgO slices, rather than the freshly cleaved substrates used in the present work, and the apparent facetting may have been due to slightly off-axis substrates or growth in a $p_w : p_B$ ratio outside the limited range of good growth.

2.2.2. Closed System

The variation of thickness with reaction temperature between 500 and 680° C, at a nominal water vapour pressure of 25 mm, for the closed system, is given in curve *B* of fig. 1. Less initial bromide was used than in the open system, to prevent sealing of the enclosure. 0.55 g gave a deposit mass of 0.023 g at T_M representing an efficiency of 20%. The general shape of the curve is similar to that for NiO [3], and since T_M is lower than

for the open system, the melting of the $CoBr_2$ is less important.

The deposit thickness was not uniform over the whole growth range, as for NiO the deposit being thicker, at low temperatures, at the centre of the substrate, and above T_M being thicker at the edges. The reasons again being a modification of the $p_W : p_B$ ratio at the substrate surface due to the enclosed nature of the system.

In conclusion, it is evident that epitaxial single crystals of CoO can be grown up to considerable thicknesses by single deposition, much greater, in fact, than reported by other workers, providing the experimental system and growth parameters are correctly chosen.

3. Structural Perfection

3.1. Experimental

Many etching solutions were tried in an attempt to examine the CoO overgrowth and the MgO substrate separately, in a manner similar to that used by the present authors in the examination of epitaxial NiO single crystals [3]. In the NiO case, it was possible to remove the substrate and examine the interfacial surface of the overgrowth, but for epitaxial CoO it proved impossible to remove the substrate. All the etchants used attacked the CoO and the MgO to about the same degree, and the most satisfactory etchant for both overgrowth and substrate proved to be a solution consisting of five parts saturated ammonium chloride, one part concentrated sulphuric acid and one part distilled water. Dislocation arrays were revealed after a 15 min etch at room temperature, but only the growth surface and CoO/MgO cross-sections could be examined, the latter by first cleaving the crystals normal to the growth surface.

X-ray topographs were taken with $CoK\alpha$ radiation using {420}, {400} or {311} reflections and the Berg : Barrett technique [7], under the experimental arrangement described in a previous paper [2].

Crystals were examined both optically and topographically in the as-grown state and after annealing at 1350° C in a low pressure argon atmosphere.

3.2. Observations

The bulk perfection of CoO varied considerably over the range of growth temperatures investigated, although no cleavage or gross plastic deformation at the interface common to NiO/MgO [3] was observed. At low temperatures and consequently low thicknesses, only random arrays of etch pits were seen on the growth surfaces, and both the MgO and CoO cross-sections (dislocation density at least two orders of magnitude greater in the CoO). As the growth temperature increased above 600° C however, isolated ⟨100⟩ slip traces were observed optically and topographically on the growth surfaces. As the crystal thickness increased in the vicinity of T_M, the slip became extensive, and macroscopic slip covered the whole growth surface (fig. 2). Etching these latter cross-sections revealed a dense array of short ⟨110⟩ traces in the immediate vicinity of the growth surface (fig. 3). As the thickness decreased beyond T_M, the slip network in the growth surface became less extensive again, but the ⟨110⟩ slip traces in the cross-section of the CoO extended further into the bulk of the crystal. At the highest growth temperatures (> 715° C) isolated ⟨110⟩ slip lines were observed at the interface, although there was still no accompanying slip in the MgO. Topographs from the growth face illustrated the concave curvature of the CoO, which was very marked in thick crystals.

The overall dislocation density in the growth surfaces was difficult to measure absolutely because (i) the individual pits were not clearly defined, (ii) the density was very high, and (iii) in many instances, the surface morphology prevented examination at high magnifications. However, it was estimated that the dislocation density in the growth surface was greater than $10^8/cm^2$, and observations of etched cross-sections showed that the density was a maximum at the growth surface and a minimum at the interface.

In addition to random arrays of dislocations and occasional slip lines, the etched cross-sections revealed clear striations (fig. 4) in crystals of all thicknesses, grown over the entire temperature range. These striations were parallel to the interface close to the interface, but basically followed the contours of the growth surface. They were clearly revealed topographically, and, in addition, the topographs showed that there was some misorientation (considerable in the case of the thick crystals) associated with these striations.

Annealing the CoO/MgO crystals at 1350° C removed all the plastic deformation near the growth surface and the striations in the bulk, and the topographs showed that the overall curvature had been considerably reduced. Etching revealed that the overall dislocation

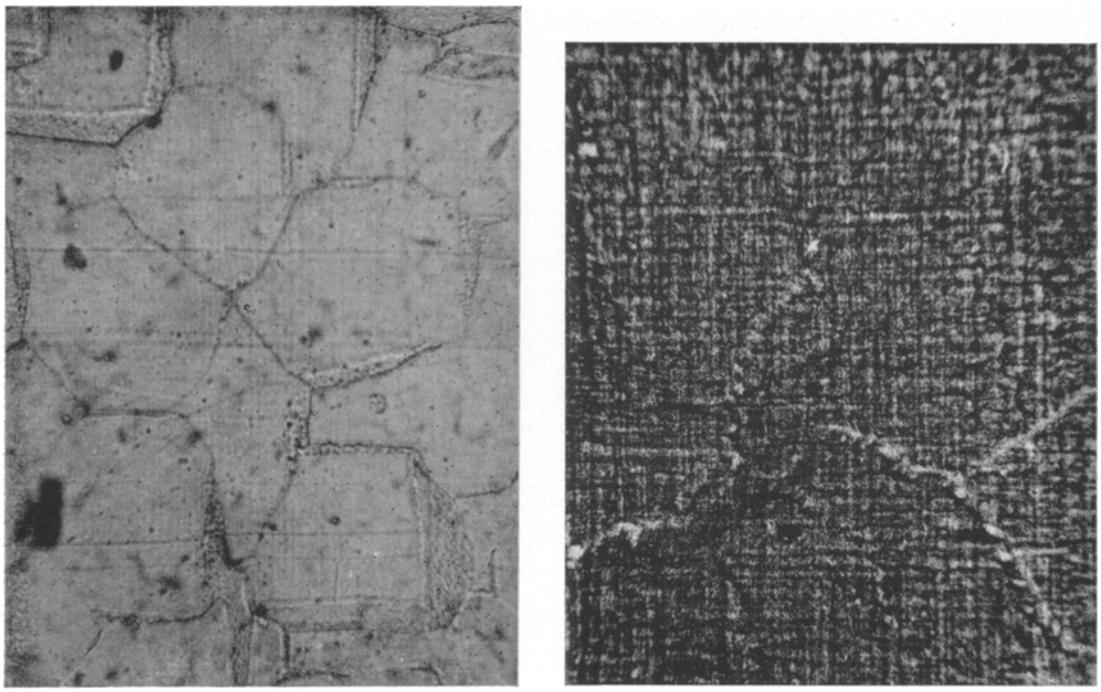

(a) (b)

Figure 2 Macroscopic slip in the growth surface of cobalt oxide grown at high temperature (a) optical micrograph (× 735), and (b) X-ray topograph (× 40).

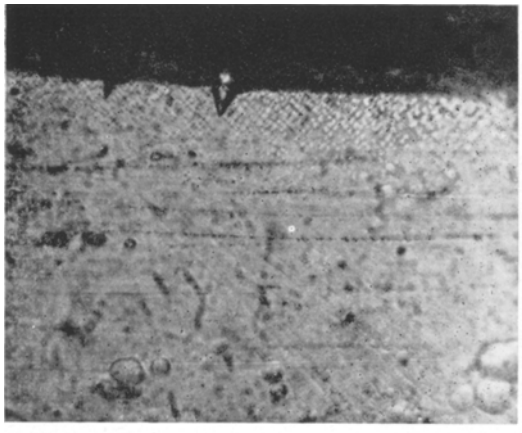

Figure 3 Etched cross-section of CoO showing ⟨110⟩ slip traces near the growth surface (× 610).

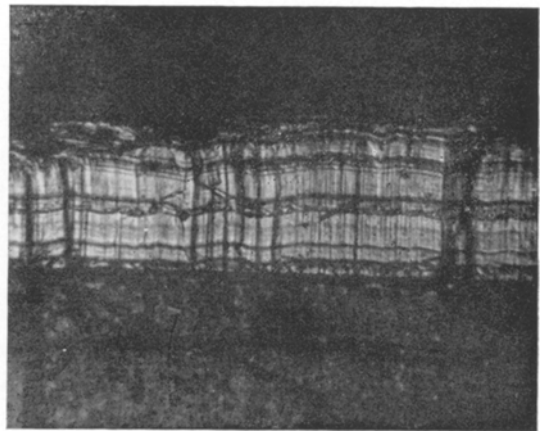

Figure 4 Growth striations in the cross-section of CoO revealed by etching (× 43).

density in the growth surface had been reduced by a factor of ten (to about $10^7/cm^2$), and that the density in the cross-section appeared to be a maximum in the centre of the overgrowth, and a minimum near the interface and the growth face. Optical examination revealed that the interface itself was somewhat diffuse, suggesting that considerable diffusion of CoO across the interface had occurred during annealing. Topographs from the edges showed that the misorientation associated with the striations had been removed, and confirmed the diffuse nature of the interface. Further evidence for diffusion on annealing was that regions of MgO previously uncovered with growth, were now lightly coated with CoO.

3.3. Discussion on Structural Perfection

It is of interest to compare the results of this

work on CoO with that on NiO [3]. The dominant features associated with these CoO crystals are: (i) concave curvature of the crystal (identical to NiO); (ii) dislocation networks near the growth surface (at the interface in both NiO and MgO); (iii) striations (not observed in NiO); (iv) absence of cleavage (prominent in NiO/MgO, both normal and parallel to the substrate).

It was emphasised in [3] that the concave curvature of the epitaxial films was a consequence of differential thermal contraction between the substrate and the deposit, and not due to lattice mismatch. This is further confirmed in the present work since $a_{CoO} > a_{MgO}$ compared with $a_{NiO} < a_{MgO}$, yet the observed curvature is the same. The stress at the interface (σ_f) due to the differences in thermal expansion coefficient is found from a similar analysis to that used for NiO [3]. The calculated values of σ_f are 3.6 and 0.4 kg/mm^2 for MgO and CoO respectively, which are less than the respective critical shear stresses (σ_c), and are insufficient to produce slip. This agrees with the observation that no slip is observed at the interface. The considerable difference between σ_f for NiO/MgO and CoO/MgO is largely due to the Néel temperature of NiO (and the associated anomalies in physical properties), which occurs well above room temperature, whereas that for CoO does not. Although it is difficult to analyse completely the stress distribution in a thick overgrowth strained in tension on a thick substrate, it would be expected that the stress is a maximum at the interface. Thus, if differential thermal contraction cannot produce slip at the interface, it cannot possibly produce it at the growth surface, as observed. Therefore, some additional stress must be present which was absent or masked by the high interfacial stress in the case of NiO/MgO.

The only experimental observation in CoO not evident in NiO was of the striations on the cross-sections of the crystals, and since these follow the surface contours, they are undoubtedly associated with the growth process. Growth striations are a common feature in melt grown crystals and are a result of the segregation of defects/impurities produced by thermal fluctuations in the melt or artificial changes in the growth rate. Since the surface morphology has been shown to be extremely dependent on the $p_W : p_B$ ratio, it is likely that the striations are also dependent on this ratio. During a growth run of several hours it is unlikely that the experimental conditions remain completely stable owing to slight variations in water vapour pressure in the vicinity of the substrate, and the increasing diffusion path of the bromide vapour as the level of the bromide powder decreases. Changes in either of these parameters will alter the growth rate and possibly lead to variations in the defect/impurity density. Similar striations would not be expected to occur so readily in NiO, since the surface morphology (and growth characteristics) are less susceptible to slight changes in the $p_W : p_B$ ratio. Changes in defect/impurity density will lead to stress in the bulk of the CoO, and as shown by Bonse [8] in his observations of growth striations in quartz, stress relief will occur at the surfaces. Since the lower face of the CoO is restrained by the MgO substrate, stress relief can only occur at the free surface and this may well account for the observed slip near the surface. The slip is more marked in thicker crystals because the bulk stress induced during growth will be greater. The absence of cleavage in CoO/MgO must be a direct result of the low interfacial stress produced by differential thermal contraction.

Annealing the crystals removes the striations and their associated misorientations, and on cooling, the only stress remaining is that due to thermal contraction. This stress has been shown to be sufficient to induce slip but maintains the concave curvature of the crystals which is less marked than before annealing, due to the removal of bulk stress. Furthermore, the diffusion of CoO across the interface means that the interfacial stress will be less localised after annealing and even less likely to produce slip. This is in accordance with the experimental observations in that no plastic deformation whatsoever, is seen in either the CoO or MgO after annealing. Annealing allows many defects to diffuse out of the crystal and explains why the dislocation density near the surface is much less than that in the bulk of the crystal.

4. Antiferromagnetic Domain Structure

As stated previously, CoO single crystals, below the Néel temperature, may be composed of domains and possible twin walls because of the tetragonal distortion. Since any one of the three cubic axes can be the contraction axis, there are three possible types of antiferromagnetic domain. For convenience, these will be designated I, II and III corresponding to [100], [010] and [001] contraction axes respectively, (the [001] direction being normal to the (001) MgO interface). The only possible T walls between

these domains are of the {1 1 0} type, and between any pair of domains there are two possible T walls, namely:

Domains	I–II		I–III		II–III	
T walls	(1 1 0)	(1$\bar{1}$ 0)	(1 0 1)	($\bar{1}$ 0 1)	(0 1 1)	(0 $\bar{1}$ 1)

No T walls are common to different pairs of domains, and walls separating one pair of domains cannot intersect those separating another pair without the introduction of considerable lattice misfit and strain. There is no analogy to the strain free four-wall structure of NiO, where all four domains can meet in a single line. Although no theoretical study has been made of the wall thickness and energy associated with domains in CoO, it is likely that they will be of similar magnitude to the {1 1 0} walls in NiO [9], since there must be a similar spin rotation associated with the walls.

4.1. Experimental

The CoO crystals were examined optically and topographically while still attached to the substrate, the optical examination being restricted to crystals less than about 75 μm thick because of the high absorption. Crystals were examined in the as-grown state and after annealing at 1300° C, and to study the domain behaviour it was necessary to cool the specimens well below the Néel temperature.

Optical observation between crossed polars was achieved by using a low-temperature microscope stage (transmitted light) similar to that described by Rhodes [10], and the temperature could be continuously controlled down to −125° C. Since the domains were most clearly revealed at lowest temperatures, X-ray topographs were taken at room temperature and at about −100° C, using a liquid nitrogen cold finger. The low temperature arrangement meant that the photographic plate could not be placed as close to the specimen surface as in the observation of NiO, which reduced the resolution resulting in less sharp topographs than their NiO counterparts.

4.2. Observations on Domains

4.2.1. Optical Observations of As-grown Crystals

At room temperature, the CoO crystals were isotropic and almost black under crossed polars, but as the crystals cooled below T_N, faint, slightly lighter, narrow lamellar domains became visible, reaching maximum clarity below −100° C. These lamellar domains were parallel to ⟨1 1 0⟩ and generally appeared in groups of at least two, randomly distributed throughout the crystal (fig. 5). The individual domains in the group were separated by sharp lines parallel to ⟨1 1 0⟩, but the overall group was separated from the dark background by rather diffuse boundaries. Maximum contrast was obtained with the incident beam polarised along ⟨1 1 0⟩, and no reversal in intensity was seen as the crystal was rotated through 90°. The matrix of the crystal was always dark (optic axis and hence contraction axis normal to the interface) and the lamellar domains always light (optic axis in the interface). Repeated heating to room temperature and subsequent cooling to −100° C did not alter the domain structure.

The width and length of the lamellar domains increased with increasing crystal thickness, from $<3\,\mu$m at a thickness of 10 μm up to about 10μm at a thickness of 60 μm (fig. 5). Due to the high optical absorption, it could not be ascertained whether the domains continued to increase in size in crystals thicker than about 75 μm.

4.2.2. Topographic Observations on As-grown Crystals

In general, the individual domains were too numerous, and the overall domain structure too complex, for topographical resolution. Only general features such as gross curvature and networks of small angle boundaries were observed. However, in some crystals thicker than 150 μm, a few isolated ⟨1 1 0⟩ domains could be seen, proving that the domains continued to increase in size as the crystal thickness increased.

Although the topographs gave little information on the individual domains, the overall intensity of the reflection was used to investigate the relative proportions of the crystal that had contracted normal or parallel to the interface. Topographs were taken from the (0 0 1) growth face with [1 0 0] vertical, using the (0 2 $\bar{4}$) reflections, but, as was the case for NiO, these indices define a set of planes in a single domain, and there is a change in Bragg angle, as well as a relative misorientation, between the equivalent planes in different domains. Using known lattice constants of CoO [1, 11], the net result is that at −100° C domains I and II should reflect 6′ away from one another (virtually coincident) and 1° 25′, away from domain III.

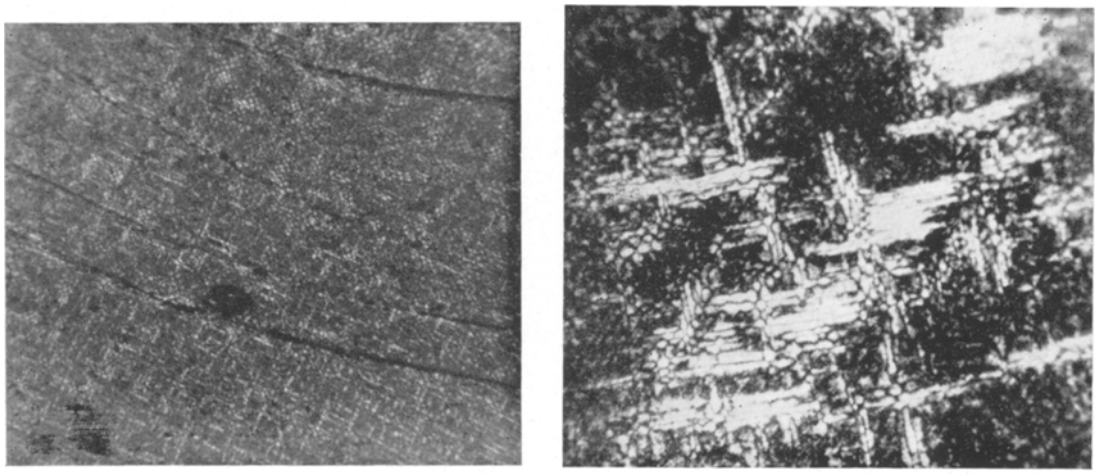

(a) (b)

Figure 5 Lamellar type I and II domains distributed on a basic type III domain matrix in (a) a crystal 15 μm thick, and (b) a crystal 60 μm thick ($\times$ 66).

Experimental observations of all the CoO crystals revealed that there were, in fact, two angular settings for the $(02\bar{4})$ reflection at low temperatures, and that their angular misorientation was approximately 1° 25′, confirming that the magnitude of the tetragonal distortion in epitaxial CoO is the same as that in melt-grown crystals. The intensities of each pair of topographs showed that there was always more of type III domain, with the contraction axis normal to the interface, than that of type I and II combined, the percentage of type III being between 55 and 65%.

4.2.3. Effects of Annealing on the Domain Structure

After annealing at 1300° C, the domain structure was re-examined optically and topographically, and was found to be very similar to that observed prior to annealing, unlike NiO, where annealing produced a very regular low energy configuration with all the domains bounded by crystallographic T walls. The average domain size in CoO became much smaller, with a more homogeneous distribution, with the result that domains were never resolved topographically whatever the crystal thickness. However, the proportion of domain III to types I and II was still about 3:2.

4.3. Discussion of the Twin Domain Structure

The optical and X-ray observations both indicated that, below T_N, the crystals consisted of a type III domain matrix with lamellar $\langle 1\,1\,0 \rangle$ type I and II domains distributed throughout the matrix, but neither technique differentiated between types I and II.

Before considering the individual domains in detail, the overall density of type III to type I and II domains will be discussed. From the observations on epitaxial NiO crystals, where the presence of the substrate was shown to be the major factor controlling the domain structure, the tetragonal contraction of CoO might be expected to occur normal to the surface over the entire crystal. This would maintain the "square" symmetry at the interface, and the increase in the lattice parameters in the interface could relieve the tensile stress in the CoO caused by differential thermal contraction between the CoO and MgO. However, at $-100°$ C, the increase in lattice constant due to the distortion over-compensates the tensile stress induced by cooling from the growth temperature (assuming an isotropic expansion coefficient for CoO below T_N). Thus the introduction of randomly distributed type I and II domains would be expected in order to maintain an equilibrium condition.

The percentage of type I and II domains necessary to completely eliminate the interfacial stress at $-100°$ C due to differential thermal contraction can be estimated as follows. If growth is assumed to occur in a strain-free environment at 620° C (T_G) and the crystal is then cooled to $-100°$ C (T_0), the interfacial strain between the CoO and MgO is $2\,\Delta\alpha(T_G -$

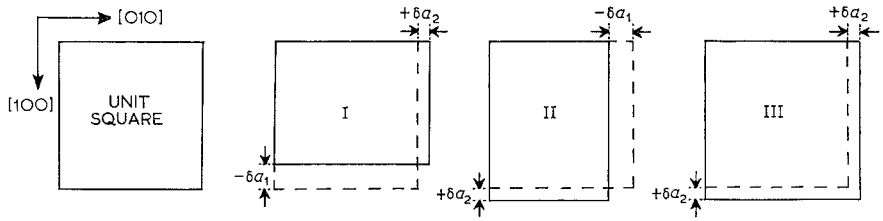

Figure 6 Configuration of the various domains relative to a square matrix at −100° C.

T_0) A, where $\Delta\alpha$ is the difference in expansion coefficients and A is the surface area of the interface. Allowing for the anomalous behaviour of α in the vicinity of T_N for CoO, this gives approximately 2.0×10^{-3} A. Due to the tetragonal distortion, different domains will have different configurations in the interface, and fig. 6 shows that at −100° C, type III domains tend to increase the interfacial area of the CoO, whereas type I and II domains tend to decrease it (δa_1 and δa_2 are unit expansion or contraction in fig. 6). If x is the fraction of domain III and y the combined fraction of type I and II in the interface, then $x + y = 1$. Now, equating the overall tensile strain in the interface due to differential thermal contraction, against the net increase in surface area at −100° C due to the tetragonal distortion (using the known lattice constants [1, 11] and neglecting elemental areas) gives:

$$2 \times \delta a_2 A - y(\delta a_1 - \delta a_2) A = 2 \times 10^{-3} A .$$

Substituting for x or y gives $y = 0.45$ and $x = 0.55$.

Therefore the percentage of type I and II domains required to completely eliminate the interfacial stress at −100° C is 45%. This agrees with the experimental value obtained from the density of the low temperature topographs, confirming that the formation of types I and II domains is predominantly associated with the lowering of the interfacial stress. However, the low temperature topographs showed that the CoO was still curved concavely, indicating that the tensile stress had not been completely relieved. This suggests that the overall tensile stress in the CoO must be somewhat greater than that calculated solely in terms of differential thermal contraction.

Returning to the individual domains, the optical observations show that the I and II domains occur as groups of narrow lamellae parallel to ⟨1 1 0⟩. The sharp lines separating the individual lamellae are undoubtedly T walls running normal to the interface and are boundaries between I and II domains. Since these domains are necessary to reduce the overall stress at the interface, as discussed above, it is energetically favourable for these to occur in groups of at least two, as this relieves the stress isotropically in the interface (see fig. 7). Furthermore, because these lamellar domains are separated from one another, within a given group, by crystallographic T walls normal to the interface, it is easy to see why they are narrow. There is an angular misorientation in the interface associated with the T walls (fig. 8), and the additional induced stress can only be minimised by the formation of narrow domains (similar to NiO [2]). This restriction on domain width decreases as the crystal thickness increases, because the effect of the interface on the bulk of the crystal becomes less marked, and accounts for the increase in domain width as the crystal thickness increases.

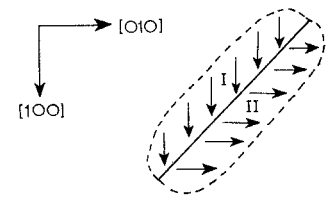

Figure 7 Schematic representation of a type I/II domain, separated by a {1 1 0} T wall, showing the relative contraction axes.

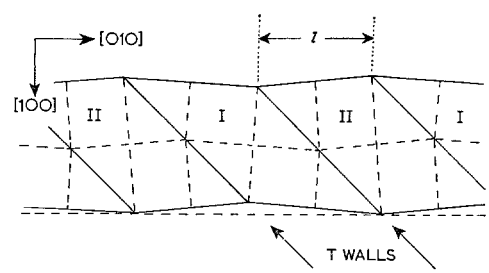

Figure 8 Angular misorientation associated with adjacent domains type I and II, viewed normal to the interface (exaggerated for effect).

Although the boundaries between domains within a group were very sharp, the overall boundaries of the groups were somewhat diffuse. The reason for these diffuse boundaries is that the ⟨1 1 0⟩ lamellar I and II domains must be separated from the surrounding type III matrix with considerable lattice misfit, since crystallographic T walls between I (or II) and III would have ⟨1 0 0⟩ traces in the surface, and these were never observed. The lamellar domains occur parallel to ⟨1 1 0⟩ rather than ⟨1 0 0⟩ since the stress relief for type I and II domains occurring in groups separated by T walls normal to the interface, must overcome the stress associated with the non-crystallographic boundaries surrounding the groups.

In as-grown crystals, the distribution of the lamellar domains is random and basically governed by regions of excessive stress incorporated into the bulk of the growing crystal, since successive heating to room temperature and subsequent cooling does not alter their distribution. Annealing at 1300° C must remove regions of localised stress, resulting in a more homogeneous distribution of smaller domains, whose appearance is almost completely controlled by the substrate.

5. Conclusions

Cobalt oxide single crystals can be grown epitaxially onto (0 0 1) cleavage faces of MgO over a wide temperature range, producing uniformly thick crystals of good quality, providing that the ratio of bromide to water vapour pressure is correctly chosen. The crystals are similar to those of NiO grown by the same technique, but the surface morphology is more susceptible to small changes in this vapour pressure ratio.

Although the mismatch between overgrowth and substrate is positive, whereas it is negative in NiO, the CoO crystals still have a concave curvature (even after annealing) proving that induced stresses due to lattice mismatch are minimal compared to those due to differential thermal contraction.

There is no macroscopic deformation at the interface or gross cleavage, as was found for NiO, largely due to the fact that the Néel temperature for CoO is much lower, resulting in much lower induced stress as the crystals cool from the growth temperature. However, slip networks are observed near the growth surface of thick crystals grown near T_M, and are a result of the additional induced stress in the bulk of the crystals due to growth striations.

The antiferromagnetic domain structure in CoO is shown to be directly influenced by the substrate, as was the case in NiO, but is necessarily more complex in CoO, due to the nature of the antiferromagnetic distortion and the formation of only three types of domain. The tetragonal distortion is unaffected by the presence of the substrate, and the associated strain energy is accommodated by the formation of narrow domains of type I and II in a basic type III matrix.

Annealing removes most of the plastic deformation and the growth striations, resulting in a more homogeneous distribution of the antiferromagnetic domain structure.

References

1. N. C. TOMBS and H. P. ROOKSBY, *Nature* **165** (1950) 442.
2. M. W. VERNON and F. J. SPOONER, *J. Materials Sci.* **2** (1967) 415.
3. *Idem, ibid* **4** (1969) 112.
4. R. E. CECH and E. I. ALLESSANDRINI, *Trans. Amer. Soc. Met.* **51** (1959) 56.
5. L. B. ROBINSON, W. B. WHITE, and R. ROY, *J. Materials Sci.* **1** (1966) 336.
6. J. H. GREINER, A. E. BERKOWITZ, and J. E. WEIDENBORNER, *J. Appl. Phys.* **37** (1966) 2149.
7. W. BERG, *Z. Krist.* **89** (1934) 286; C. S. BARRETT, *Trans. AIME* **161** (1945) 15.
8. U. BONSE, *Z. Physik* **184** (1965) 71.
9. T. YAMADA, *J. Phys. Soc. Japan* **21** (1966) 650.
10. R. G. RHODES, *J. Sci. Instr.* **27** (1950) 333.
11. S. GREENWALD, *Acta Cryst.* **6** (1953) 396.